PCCP

Homogeneous nucleation and the Ostwald step rule

Pieter Rein ten Wolde and Daan Frenkel

FOM Institute for Atomic and Molecular Physics, Kruislaan 407, 1098 SJ Amsterdam, The Netherlands

Received 30th November 1998, Accepted 26th February 1999

We compare the pathways for homogeneous nucleation in a number of different systems. In most cases, the simulations show that the nucleation pathways are markedly different from what is assumed in classical nucleation theory. We find that homogeneous nucleation exhibits, at the microscopic level, features that were formulated over a century ago by Ostwald to account for the nucleation of metastable bulk phases. We observe that the structure of the precritical nuclei may differ qualitatively from that of (post)critical nuclei. Surprisingly, in the interface of the larger nuclei, traces of the structure of the smaller nuclei survive.

I Introduction

It is well known that liquids can be supercooled before they freeze and vapors can be supersaturated before they condense. In the early eighteenth century, Fahrenheit[1] found that boiled water could be kept overnight at a temperature of −9 °C (16 °F) without freezing. Only when small ice particles were introduced was the crystallization process initiated and the temperature of the ice–water mixture rose to 0 °C, the "freezing" point of water. At the end of the last century Ostwald[2] noted that highly supercooled melts, which he called 'labil', crystallize spontaneously, whereas weakly undercooled liquids, which he called 'metastabil', only crystallize after, for instance, 'ein leises Überstreichen eines Menschenhaares'.

A vapor, and similarly, a liquid, can be supercooled because the only route to the more stable state is *via* the formation of small *nuclei*.† The free energy of such nuclei is determined not only by the difference in chemical potential between vapor and liquid, which drives the nucleation process, but also by the surface free energy. The surface free energy term is always positive, because of the work that must be done to create an interface. Moreover, initially this term dominates and hence the free energy of a nucleus increases with size. Only when the droplet has reached a certain "critical" size, the volume term takes over, and the free energy decreases. It is only from here on that the nucleus grows spontaneously into a bulk liquid.

Gibbs[3] was the first to realize that the stability of a phase is related to the work that has to be done in order to create a critical nucleus of the new phase. However, the relevance of his work to nucleation remained largely unnoticed until the 1920s and 1930s when Volmer and Weber,[4] and Becker and Döring[5] laid the foundations for what is now called classical nucleation theory. In classical nucleation theory (CNT) it is assumed that the nuclei are compact, spherical objects, that behave like small droplets of bulk phase. The free energy of a spherical liquid droplet of radius R in a vapor is then given by

$$\Delta G = 4\pi R^2\gamma + \frac{4}{3}\pi R^3\rho\ \Delta\mu \qquad (1)$$

where γ is the surface free energy, ρ is the density of the bulk liquid, and $\Delta\mu$ is the difference in chemical potential between bulk liquid and bulk vapor. Clearly, the first term on the right hand side of eqn. (1) is the surface term, which is positive, and the second term is the volume term, which is negative; the difference in chemical potential is the driving force for the nucleation process. The height of the nucleation barrier can easily be obtained from the above expression, yielding

$$\Delta G^* = \frac{16\pi\gamma^3}{3\rho^2\Delta\mu^2} \qquad (2)$$

This equation shows that the barrier height depends not only on the surface free energy γ (and the density ρ), but also on the difference in chemical potential $\Delta\mu$. The difference in chemical potential is related to the supersaturation. Hence, the height of the free-energy barrier that separates the stable from the metastable phase depends on the degree of supersaturation. At coexistence, the difference in chemical potential is zero, and the height of the barrier is infinite. Although the system is equally likely in the liquid and vapor phase, once the system is one state or the other, the system will remain in this state; it simply cannot transform into the other state.

Macroscopic thermodynamics dictates that the phase that is formed in a supersaturated system is the one that has the lowest free energy. However, nucleation is an essentially dynamic process, and therefore one cannot expect *a priori* that, on supersaturating the system, the thermodynamically most stable phase will be formed. In 1897, Ostwald[2] formulated his step rule, stating that the crystal phase that is nucleated from the melt need not be the one that is thermodynamically most stable, but the one that is closest in free energy to the fluid phase. Stranski and Totomanow[6] reexamined this rule and argued that the nucleated phase is the phase that has the lowest free-energy barrier of formation, rather than the phase that is globally stable under the conditions prevailing. In experiments on rapidly cooled melts, nucleation of metastable phases is often found.[7–9] However, all these studies consider the formation of *bulk* phases. The simulation results discussed in this article suggest that even on a *microscopic* scale, something similar to Ostwald's step rule seems to hold.

II Homogeneous crystal nucleation from the melt

Alexander and McTague[10] have argued, on the basis of Landau theory, that at least for small supercooling, nucleation of the body-centered cubic (bcc) phase should uniquely be

† We will not consider large supersaturations, *i.e.* we will not discuss spinodal decomposition.

favored in all simple fluids exhibiting a weak first order phase transition. Also a theoretical study by Klein and Leyvraz[11] suggests that a metastable bcc phase can easily be formed from the undercooled liquid. Experimentally, nucleation of a metastable bcc phase has been observed in rapidly cooled metal melts.[7–9] However, when attempts were made to investigate the formation of metastable bcc nuclei on a microscopic scale, using computer simulation,[12–18] the picture that emerged gave little support for the Alexander–McTague scenario. For the Lennard-Jones system, which is known to have a stable face-centered cubic (fcc) structure up to the melting curve, the formation of a metastable bcc phase was observed in only one of the simulation studies reported,[13] while all other studies[12,14–18] found evidence for the formation of fcc nuclei. Of particular interest is the simulation of Swope and Andersen[18] on a system comprising one million Lennard-Jones particles. This study showed that, although both fcc and bcc nuclei are formed in the early stages of the nucleation, only the fcc nuclei grow into larger crystallites. It should be noted however, that in all these simulation studies, large degrees of supercooling (down to 50% of the melting temperature, or lower) had to be imposed to see any crystal formation on the time-scale of the simulation. For such a large undercooling one should expect the free-energy barrier for nucleation into essentially all possible crystal phases to be quite small. It is therefore not obvious that crystal nucleation at large undercooling will proceed in the same way as close to the freezing point.

We have studied homogeneous nucleation in a Lennard-Jones system closer to the freezing point, at 20% of below the melting point. As we show below, at this degree of supercooling the barrier is significant and the "brute-force" approach, where we wait for nuclei to form spontaneously, will not work. Instead, we have used the umbrella-sampling technique[19] to compute the free-energy barrier to crystal nucleation. The umbrella sampling technique can be used even at small (*i.e.* realistic) undercooling where the straightforward molecular dynamics technique will fail, because the nucleation barrier diverges at coexistence. Moreover, the umbrella-sampling technique allows us to stabilize the critical nucleus and study its structure in detail.

The basic idea of the umbrella-sampling technique is that we can sample states even near the top of the barrier by biasing the sampling of configuration space and correcting for the bias afterwards. We can bias the sampling of configuration space by adding a fictitious potential to the potential-energy function of our model system. In the present case, the biasing potential was taken to be a function of the order parameter Q_6, as introduced by Steinhardt *et al.*[20] The value of this global order parameter is a measure for the long-range orientational order and hence for the degree of crystallinity in the system. On the other hand, Q_6 is fairly insensitive to the differences between the possible crystalline structures. This implies that by using this order parameter as our reaction coordinate, we do not favor one crystalline structure over the other. Rather, the system is allowed to select its 'own' specific reaction path from the liquid to the solid.

The Gibbs free energy, G, is a function of this order parameter

$$\beta\Delta G(Q_6) = \text{constant} - \ln[P(Q_6)] \qquad (3)$$

where $\beta \equiv 1/k_B T$ is the inverse temperature, with k_B Boltzmann's constant and T the absolute temperature, and $P(Q_6)$ the probability per unit interval to find the order parameter around a given value of Q_6. We have computed the free-energy barrier by measuring the probability distribution function $P(Q_6)$ at two different pressures.[21,22] Fig. 1 shows the free-energy barriers computed for these two pressures.

Let us now consider the structure of the nuclei. An analysis of the Voronoi signatures and the bond-order parameters as

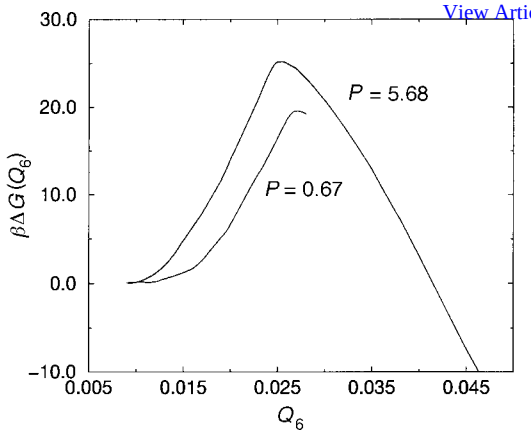

Fig. 1 The Gibbs free energy of a Lennard-Jones system as a function of crystallinity (Q_6) at 20% undercooling for two different pressures, *i.e.* $P = 5.68$ ($T = 0.92$) and $P = 0.67$ ($T = 0.6$). The temperatures and pressures are in units of the Lennard-Jones well depth ε and the Lennard-Jones diameter σ.

introduced by Steinhardt *et al.*,[20] indicated that the small crystallites in the metastable liquid are mainly bcc-ordered, whereas the postcritical nuclei are predominantly fcc-ordered.‡ In the metastable liquid we also found some small icosahedral clusters, but these did not grow into larger crystallites. We therefore determined on the basis of the distribution of the local bond-order parameter values, the fraction of particles that are in an fcc-, bcc- or liquid-like environment, denoted by f_{fcc}, f_{bcc} and f_{liq}, respectively.[22]

Fig. 2 shows the structural "composition" of the largest cluster in the system, as a function of the "reaction coordinate", Q_6. The figure shows that the precritical nuclei are predominantly bcc- and liquid-like. However, near the top of the barrier, at $Q_6 = 0.025$, there is a clear change in the nature of the solid nuclei from bcc- and liquid-like to mainly fcc-like. The fact that the precritical nuclei are rather liquid-like is not surprising as they are quite small and consist of nearly only interface. The important point to note is that these nuclei have clearly more bcc than fcc character. This suggests that, at least for small crystallites, we find the behavior predicted by Landau theory.[10] Yet, as the critical and postcritical clusters are predominantly fcc-like, the present results are also

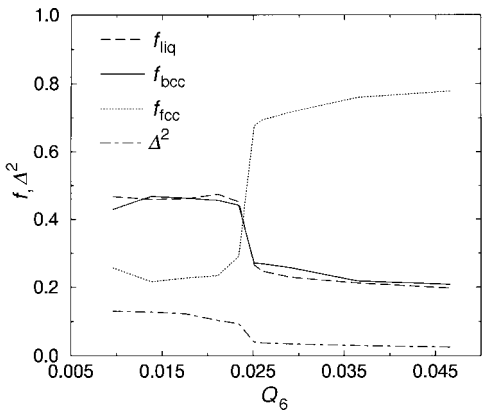

Fig. 2 Structural composition of the largest cluster in a Lennard-Jones system, indicated by f_{liq}, f_{bcc}, f_{fcc} and Δ^2, as a function of Q_6 (the reaction coordinate) at 20% undercooling ($P = 5.68$, $T = 0.92$). Δ^2 is a measure for the fraction of particles, the structure of which could not be identified as either being liquid-like, bcc-like, or fcc-like.

‡ An examination of the order parameter W_4 revealed that mainly an fcc structure is formed, rather than an hcp structure, although the difference in free energies between the two structures is small. For a more detailed study of the competition of the formation of the fcc phase *versus* the hcp phase, we would like to refer to ref. 23.

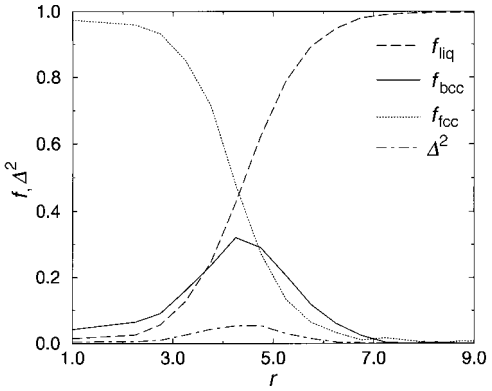

Fig. 3 Structure of the critical nucleus, indicated by f_{liq}, f_{bcc}, f_{fcc} and Δ^2, as a function of r, the distance to its center-of-mass, at 20% undercooling ($P = 5.68$, $T = 0.92$) in a Lennard-Jones system.

compatible with the findings of Swope and Andersen,[18] who observed that nucleation proceeded through fcc crystallites.

Still, we note that the critical and postcritical nuclei are not fully fcc-ordered. They have both considerable liquid- and bcc-like character. In fact, it is not surprising that the critical nucleus has some liquid-like character. After all, it consists only of some 642 particles and has therefore a large surface-to-volume ratio. However, the bcc-like character is more intriguing. We have therefore studied the local order of the critical nucleus in more detail.

Visual inspection of the critical and postcritical nuclei showed that the nuclei at this moderate degree of undercooling are fairly compact, more or less spherical objects. Given the spherical shape of the critical nucleus it is meaningful to calculate f_{liq}, f_{bcc} and f_{fcc} in a spherical shell of radius r around the center-of-mass of the cluster. Fig. 3 shows the radial profile of the local order of the critical nucleus. As expected, we find that the core of the nucleus is almost fully fcc-ordered and that far away from the center of the nucleus, f_{fcc} decays to zero and f_{liq} approaches unity. More surprisingly however, is that f_{bcc} increases in the interface and becomes even larger than f_{fcc}, before it decays to zero in the liquid. Hence, the present simulations suggest that the fcc-like core of the equilibrated nucleus is "wetted" by a shell which has more bcc character. This finding explains why Fig. 2 shows that even fairly large nuclei do not have a pure fcc signature: there is always a residual bcc signature due to the interface. It also explains the strong bcc character of the small clusters, such as appear on the liquid side of the barrier: they are so small that their structure is strongly surface-dominated.

III Coil–globule transition in condensation of polar fluids

The formation of a droplet of water from the vapor is probably the best known example of homogeneous nucleation of a polar fluid. However, the nucleation behavior of polar fluids is still poorly understood. In fact, while classical nucleation theory gives a reasonable prediction of the nucleation rate of nonpolar substances, it seriously overestimates the rate of nucleation of highly polar compounds, such as acetonitrile, benzonitrile and nitrobenzene.[24,25]

In order to explain the discrepancy between theory and experiment, several nucleation theories have been proposed. It has been suggested that in the critical nuclei the dipoles are arranged in an anti-parallel head-to-tail configuration,[24,25] giving the clusters a non-spherical, prolate shape, which increases the surface-to-volume ratio and thereby the height of the nucleation barrier. In the oriented dipole model introduced by Abraham,[26] it is assumed that the dipoles are perpendicular to the interface, yielding a size dependent surface tension due to the effect of curvature of the surface on the dipole–dipole interaction. However, in a density-functional study of a weakly polar Stockmayer fluid, it was found that on the liquid (core) side of the interface of critical nuclei, the dipoles are not oriented perpendicular to the surface, but parallel.[27]

We have studied the structure and free energy of critical nuclei, as well as pre- and postcritical nuclei, of a highly polar Stockmayer fluid.[28] In the Stockmayer system, the particles interact *via* a Lennard-Jones pair potential plus a dipole–dipole interaction potential

$$v(\boldsymbol{r}_{ij}, \boldsymbol{\mu}_i, \boldsymbol{\mu}_j) = 4\varepsilon\left[\left(\frac{\sigma}{r_{ij}}\right)^{12} - \left(\frac{\sigma}{r_{ij}}\right)^{6}\right] - 3(\boldsymbol{\mu}_i \cdot \boldsymbol{r}_{ij})(\boldsymbol{\mu}_j \cdot \boldsymbol{r}_{ij})/r_{ij}^5 + \boldsymbol{\mu}_i \cdot \boldsymbol{\mu}_j/r_{ij}^3 \quad (4)$$

Here ε is the Lennard-Jones well depth, σ is the Lennard-Jones diameter, $\boldsymbol{\mu}_i$ denotes the dipole moment of particle i and $\boldsymbol{r}_{ij}$ is the vector joining particle i and j. We have studied the nucleation behavior for $\mu^* = \mu\sqrt{\varepsilon\sigma^3} = 4$, which is close to the value of water.

We have computed[28] the excess free energy $\Delta\Omega$ of a cluster of size n in a volume V, at chemical potential μ and at temperature T, from the probability distribution function P_n

$$\beta\Delta\Omega(n, \mu, V, T) \equiv -\ln[P(n)] = -\ln[N_n/N] \quad (5)$$

Here β is the reciprocal temperature; N_n is the average number of clusters of size n and N is the average total number of particles. As the density of clusters in the vapor is low, the interactions between them can be neglected. As a consequence, we can obtain the free-energy barrier at any desired chemical potential μ' from the nucleation barrier measured at a given chemical potential μ *via*

$$\beta\Delta\Omega(n, \mu', V, T) = \beta\Delta\Omega(n, \mu, V, T) - \beta(\mu' - \mu)n + \ln[\rho(\mu')/\rho(\mu)] \quad (6)$$

where $\rho = N/V$ is the total number density in the system.

Fig. 4 shows the comparison between the simulation results and CNT for the height of the barrier. Clearly, the theory underestimates the height of the nucleation barrier. As the nucleation rate is dominated by the height of the barrier, our results are in qualitative agreement with the experiments on strongly polar fluids,[24,25] in which it was found that CNT overestimates the nucleation rate. But, unlike the experiments, the simulations allow us to investigate the microscopic origins of the breakdown of classical nucleation theory.

In classical nucleation theory it is assumed that already the smallest clusters are compact, more or less spherical objects. In a previous simulation study on a typical nonpolar fluid, the Lennard-Jones fluid, we found that this is a reasonable assumption,[29] even for nuclei as small as ten particles.

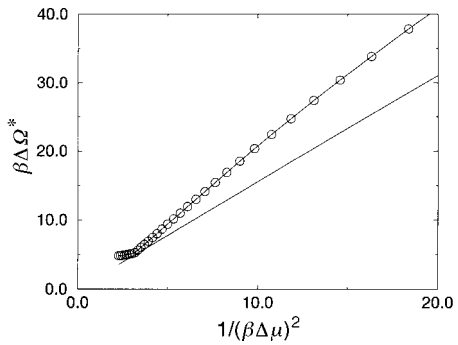

Fig. 4 Comparison of the barrier height between the simulation results (open circles) and classical nucleation theory (straight solid line) for a Stockmayer fluid with reduced dipole moment $\mu^* = \mu/\sqrt{\varepsilon\sigma^3} = 4$ and reduced temperature $T^* = k_B T/\varepsilon = 3.5$. The chemical potential difference $\Delta\mu$ is the difference between the chemical potential of the liquid and the vapor.

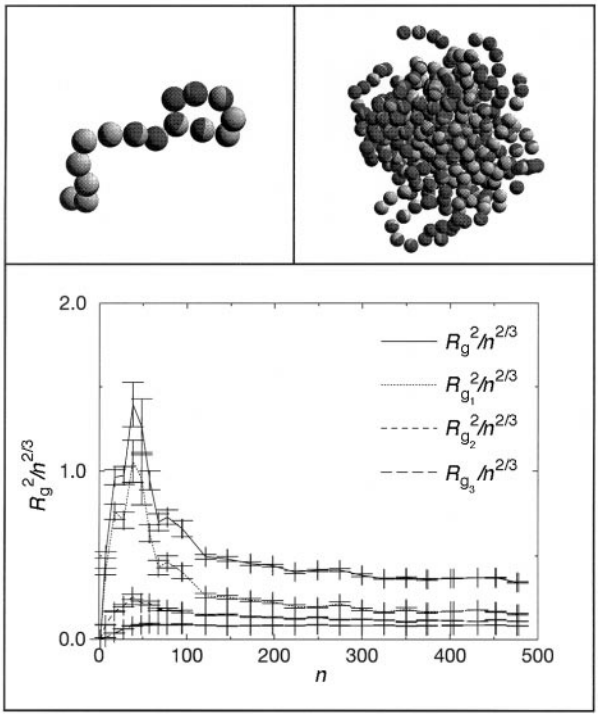

Fig. 5 Radius of gyration R_g, and the three eigenvalues of the moment-of-inertia tensor, as a function of the size n of a Stockmayer cluster, at supersaturation $S = 1.26$, temperature $T^* = 3.5$ and reduced dipole moment $\mu^* = 4$. Initially, the clusters are chain-like (snapshot top left), but at a cluster size of $n \approx 30$ they collapse to compact, spherical nuclei (snapshot top right).

However, the interaction potential of the Lennard-Jones system is isotropic, whereas the dipolar interaction potential is anisotropic. On the other hand, the bulk liquid of this polar fluid is isotropic.

We find that the smallest clusters, that initiate the nucleation process, are not compact, spherical objects, but chains, in which the dipoles align head-to-tail. In fact, we find a whole variety of differently shaped clusters in dynamical equilibrium: linear chains, branched chains, and "ring-polymers". Initially, when the cluster size is increased, the chains become longer. But, beyond a certain size, the clusters collapse to form a compact globule. In order to quantify this behaviour, we have determined the size dependence of the radius-of-gyration, as well as the three eigenvalues of the moment-of-inertia tensor. In Fig. 5 we show the square of the radius of gyration, divided by $n^{2/3}$. For a compact, spherical object R_g^2 scales with $n^{2/3}$, whereas for chains R_g^2 scales with n^{α}, where $1.2 < \alpha < 2$, depending on the stiffness of the chain. Hence, for chain-like clusters $R_g^2/n^{2/3}$ should increase with n, whereas for a globule it should approach a constant value.

Fig. 5 shows that initially $R_g^2/n^{2/3}$ increases with the size of the cluster. Moreover, one eigenvalue of the moment-of-inertia tensor is much larger than the other two, indicating the tendency of clusters to form chains. However, at a cluster size of $n \approx 30$, $R_g^2/n^{2/3}$ starts to decrease and approaches a constant value at $n \approx 200$. Analysis of the individual eigenvalues shows that at that point the clusters have collapsed to compact objects that fluctuate around a spherical shape. However, in the interface, traces of the tendency to form chains survive.

The Stockmayer fluid is a simple model system for polar fluids and the mechanism that we describe here might not be applicable for all fluids that have a strong dipole moment. The nucleation behavior of water, for instance, is probably more dominated by hydrogen bonding.[30] Still, our simulations clearly show that the presence of a strong permanent dipole can drastically change the pathway for condensation.

IV Protein crystallization

Proteins are notoriously difficult to crystallize. The experiments indicate that proteins only crystallize under very specific conditions.[31–33] Moreover, the conditions are often not known beforehand. As a result, growing good protein crystals is a time-consuming business.

In 1994, George and Wilson[34] proposed that the success of protein crystallization is correlated with the value of B_2, the second osmotic virial coefficient. The second virial coefficient describes the lowest order correction to the van't Hoff law for the osmotic pressure Π:

$$\frac{\Pi}{\rho k_B T} = 1 + B_2 \rho + (\text{terms of order } \rho^2) \qquad (7)$$

where ρ is the number density of the dissolved molecules, k_B is Boltzmann's constant, and T is the absolute temperature. The value of the second virial coefficient depends on the effective interaction between a pair of macromolecules in solution:[35]

$$B_2 = 2\pi \int r^2 \, dr[1 - \exp[-\beta v(r)]] \qquad (8)$$

where $\beta \equiv 1/k_B T$ and $v(r)$ is the interaction energy of a pair of molecules at distance r. For macromolecules, B_2 can be determined from static light scattering experiments.[36]

George and Wilson measured B_2 for a number of proteins in various solvents. They found that for those solvent conditions that are known to promote crystallization, B_2 was restricted to a narrow range of small negative values. For large positive values of B_2 crystallization did not occur at all, whereas for large negative values of B_2 protein aggregation, rather than crystallization, took place. This correlation has been extended to over 20 distinct proteins with a wide variety of crystal structures and interaction potentials.[37]

Subsequently, Rosenbaum *et al.*[37,38] established a link between the work of George and Wilson and a computer-simulation study by Hagen and Frenkel,[39] who studied the phase behaviour of colloid–polymer mixtures. In these mixtures, the polymers induce an effective attraction between the colloids. The range of the attraction depends on the radius-of-gyration of the polymer. Thus, by regulating the effective size of the polymer, the interaction range between the colloids can be tuned. Since the theoretical work of Gast *et al.*,[40,41] it is known that the range of attraction between spherical colloids has a drastic effect on the overall appearance of the phase diagram. If the range of attraction is long in comparison to the diameter of the colloids, the phase diagram of the colloidal suspension resembles that of an atomic substance, such as argon: depending on the temperature and density, the colloids can occur in three phases (Fig. 6A); a dilute colloidal fluid (analogous to the vapor phase), a dense colloidal fluid (analogous to the liquid phase), and a colloidal crystal phase. However, when the range of the attraction is reduced, the fluid–fluid critical point moves towards the triple point, where the solid coexists with the dilute and dense fluid phases. At some point, the critical point and the triple point will coalesce. If the range of attraction is made even shorter (less than some 25% of the colloid diameter), only two stable phases remain: one fluid and one solid (Fig. 6B). However, the fluid–fluid coexistence curve survives in the metastable regime below the fluid–solid coexistence curve (Fig. 6B). This is indeed found in experiments[42–45] and simulations.[39]

Why is this relevant for protein crystallization? First of all, globular proteins in solution often have short-ranged attractive interactions. In fact, a series of studies[46–49] show that the phase diagram of a wide variety of proteins is of the kind shown in Fig. 6. In addition, Rosenbaum *et al.*[37,38] showed that the phase diagrams can be mapped on top of each other when compared on equal footing, *i.e.* on the basis of the

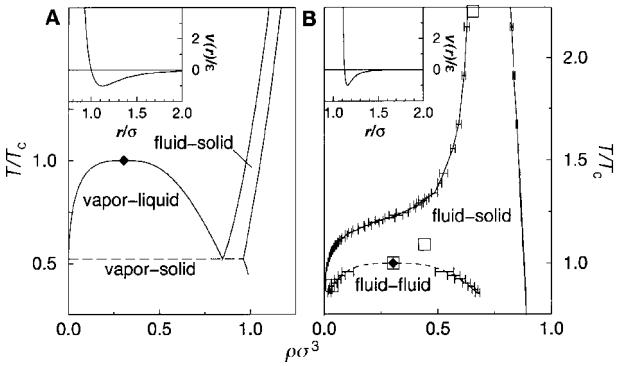

Fig. 6 (A): Typical phase diagram of a molecular substance with a relatively long-ranged attractive interaction. The phase diagram shown here corresponds to the Lennard-Jones 6-12 potential $\{v(r) = 4\varepsilon[(\sigma/r)^{12} - (\sigma/r)^6]$, solid curve in insert$\}$. The dashed line indicates the triple point. (B): Typical phase diagram of colloids with short-ranged attraction. The phase diagram was computed for the potential given in eqn. (9) (solid curve in insert), with $\alpha = 50$. In both figures, the temperature is expressed in units of the critical temperature T_c, while the number density is given in units σ^{-3}, where σ, the effective diameter of the particles is defined in the expression for $v(r)$. The diamonds indicate the fluid–fluid critical points. In both figures, the solid lines indicate the equilibrium coexistence curves. The dashed curve in B indicates the metastable fluid–fluid coexistence. Crystal-nucleation barriers were computed for the points denoted by open squares.

density and the second virial coefficient. However, the most interesting observation of Rosenbaum *et al.*[37,38] is that the conditions under which a large number of globular proteins can be made to crystallize, map onto a narrow temperature range, or more precisely, a narrow range in the value of the osmotic second virial coefficient, of the computed fluid–solid coexistence curve of colloids with short-ranged attraction.[39] If the temperature is too high, crystallization is hardly observed at all, whereas if the temperature is too low, amorphous precipitation rather than crystallization occurs. Only in a narrow window around the metastable critical point, high-quality crystals can be formed. Several authors had already noted that a similar crystallization window exists for colloidal suspensions.[50,51] We have investigated the origin of this crystallization window. We found that the presence of a metastable fluid–fluid critical point is essential.[52]

In order to grow high-quality protein crystals, the quench should be relatively shallow, and the system should not be close to a glass transition. Under these conditions, the rate-limiting step in crystal nucleation is the crossing of the free-energy barrier. We have therefore computed the free-energy barrier for homogeneous crystal nucleation for a model "globular" protein. In this model system, the particles interact *via* a modified Lennard-Jones potential

$$v(r) = \begin{cases} \infty & (r < \sigma) \\ \dfrac{4\varepsilon}{\alpha^2}\left(\dfrac{1}{[(r/\sigma)^2 - 1]^6} - \alpha\dfrac{1}{[(r/\sigma)^2 - 1]^3}\right) & (r \geqslant \sigma) \end{cases} \quad (9)$$

where σ denotes the hard-core diameter of the particles and ε the well depth. The width of the attractive well can be adjusted by varying the parameter α. Fig. 6 shows the phase diagram for $\alpha = 50$. It is clear that the potential in eqn. (9) provides a simplified description of the effective interaction between real proteins in solution: it accounts both for direct and for solvent-induced interactions between the globular proteins. However, the model system reproduces the phase behaviour of proteins in solution. In fact, the phase-diagram can be mapped onto the experimentally determined phase-diagrams of a variety of globular proteins.[37,38]

The free-energy barriers were computed for the four points denoted by open squares in Fig. 6. These points were chosen such that on the basis of classical nucleation theory the same height of the barrier could be expected. In order to compute the free-energy barrier, we have computed the free energy of a nucleus as a function of its size. However, we first have to define what we mean by a "nucleus". As we are interested in crystallization, it might seem natural to use a crystallinity criterion. However, as mentioned, we expect that crystallization near the critical point is influenced by critical density fluctuations. We therefore used not only a crystallinity criterion, but also a density criterion. We define the size of a high-density cluster (be it solid- or liquid-like) as the number of connected particles, N_ρ, that have a significantly higher local density than the particles in the remainder of the system. The number of these particles that is also in a crystalline environment, which is determined on the basis of the local bond-order parameters,[20] is denoted by N_{crys}. In our simulations, we have computed the free-energy "landscape" of a nucleus as a function of the two coordinates N_ρ and N_{crys}.

Fig. 7 shows the free-energy landscape for $T = 0.89T_c$ and $T = T_c$. The free-energy landscapes for the other two points are qualitatively similar to the one for $T = 0.89T_c$ and will not be shown here. We find that away from T_c (both above and below), the path of lowest free energy is one where the increase in N_ρ is proportional to the increase in N_{crys} (Fig. 7A). Such behavior is expected if the incipient nucleus is simply a small crystallite. However, around T_c, critical density fluctuations lead to a striking change in the free-energy landscape (Fig. 7B). First, the route to the critical nucleus leads through a region where N_ρ increases while N_{crys} is still essentially zero. In other words: the first step towards the critical nucleus is the formation of a liquid-like droplet. Then, beyond a certain critical size, the increase in N_ρ is proportional to N_{crys}, that is, a crystalline nucleus forms inside the liquid-like droplet.

Clearly, the presence of large density fluctuations close to a fluid–fluid critical point has a pronounced effect on the route to crystal nucleation. But, more importantly, the nucleation barrier close to T_c is much lower than at either higher or lower temperatures (Fig. 8). The observed reduction in ΔG^* near T_c by some 30 $k_B T$ corresponds to an increase in nucleation rate by a factor 10^{13}.

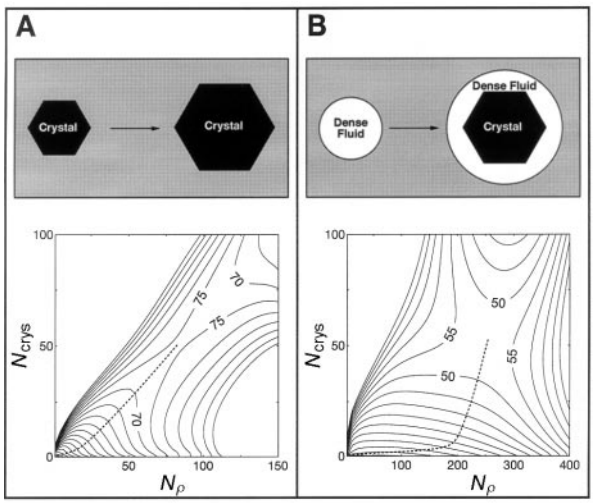

Fig. 7 Contour plots of the free-energy landscape along the path from the metastable fluid to the critical crystal nucleus, for our system of spherical particles with short-ranged attraction. The curves of constant free energy are drawn as a function of N_ρ and N_{crys} (see text) and are separated by $5k_B T$. (A): The free energy landscape well below the critical temperature ($T/T_c = 0.89$). The lowest free-energy path to the critical nucleus is indicated by a dashed curve. This curve corresponds to the formation and growth of a highly crystalline cluster. (B): As (A), but for $T = T_c$. In this case, the free-energy valley (dashed curve) first runs parallel to the N_ρ axis (formation of a liquid-like droplet), and then moves towards a structure with a higher crystallinity (crystallite embedded in a liquid-like droplet). The free energy barrier for this route is much lower than the one in (A).

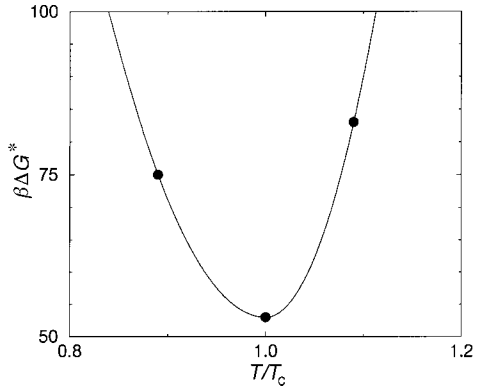

Fig. 8 Variation of the free-energy barrier for homogeneous crystal nucleation, as a function of T/T_c, in the vicinity of the critical temperature. The solid curve is a guide to the eye. The nucleation barrier at $T = 2.23T_c$ is $128k_BT$ and is not shown in this figure. The simulations show that the nucleation barrier goes through a minimum around the metastable critical point (see text).

Finally, let us consider the implications of this reduction of the crystal nucleation barrier near T_c. An alternative way to lower the crystal nucleation barrier would be to quench the solution deeper into the metastable region below the solid–liquid coexistence curve. However, such deep quenches often result in the formation of amorphous aggregates.[34,37,38,43–45,49] Moreover, in a deep quench, the thermodynamic driving force for crystallization ($\mu_{liq} - \mu_{cryst}$) is also enhanced. As a consequence, the crystallites that nucleate will grow rapidly and far from perfectly.[32] Thus the nice feature of crystal nucleation in the vicinity of the metastable critical point is that crystals can be formed at a relatively small degree of undercooling. This should lead to protein crystals of high quality. It is clear that our model is simplified. However, our model system reproduces the phase behavior of compact proteins in solution. Moreover, the mechanism that we describe here is general, and does not depend on the details of the interaction potential. We expect that when a metastable fluid–fluid coexistence is present below the stable sublimation curve, critical density fluctuations facilitate the formation of ordered structures.

V Conclusions

Ostwald formulated his step rule more than a century ago[2] on the basis of macroscopic studies of phase transitions. The simulations suggest that also on a microscopic level, a "step rule" may apply and that metastable phases may play an important role in nucleation. We find that the structure of the precritical nuclei is that of a metastable phase (bcc/chains/liquid). As the nuclei grow, the structure in the core transforms into that of the stable phase (fcc/liquid/fcc-crystal). Interestingly, in the interface of the larger nuclei traces of the structure of the smaller nuclei are retained.

Acknowledgements

This work was supported in part by 'Chemische Wetenschappen' (CW) with financial aid from NWO ('Nederlandse Organisatie voor Wetenschappelijk Onderzoek'). The work of the FOM Institute is part of the research program of "Stichting Fundamenteel Onderzoek der Materie" (FOM) and is supported by NWO.

References

1 D. B. Fahrenheit, *Philos. Trans. R. Soc.*, 1724, **39**, 78.
2 W. Ostwald, *Z. Phys. Chem*, 1897, **22**, 289.
3 J. W. Gibbs, *The Scientific Papers of J. Willard Gibbs*, Dover, New York, 1961.
4 M. Volmer and A. Weber, *Z. Phys. Chem.*, 1926, **119**, 227.
5 R. Becker and W. Döring, *Ann. Phys.*, 1935, **24**, 719.
6 I. N. Stranski and D. Totomanow, *Z. Phys. Chem.*, 1933, **163**, 399.
7 R. E. Cech, *J. Met.*, 1956, **8**, 585.
8 H.-M. Lin, Y.-W. Kim and T. F. Kelly, *Acta Metall.*, 1988, **36**, 2537.
9 W. Löser, T. Volkmann and D. M. Herlach, *Mater. Sci. Eng.*, 1994, **A178**, 163.
10 S. Alexander and J. P. McTague, *Phys. Rev. Lett.*, 1978, **41**, 702.
11 W. Klein and F. Leyvraz, *Phys. Rev. Lett.*, 1986, **57**, 2845.
12 M. J. Mandell, J. P. McTague and A. Rahman, *J. Chem. Phys.*, 1976, **64**, 3699.
13 M. J. Mandell, J. P. McTague and A. Rahman, *J. Chem. Phys.*, 1977, **66**, 3070.
14 C. S. Hsu and A. Rahman, *J. Chem. Phys.*, 1979, **71**, 4974.
15 R. D. Mountain and A. C. Brown, *J. Chem. Phys.*, 1984, **80**, 2730.
16 S. Nosé and F. Yonezawa, *J. Chem. Phys.*, 1986, **84**, 1803.
17 J. Yang, H. Gould and W. Klein, *Phys. Rev. Lett.*, 1988, **60**, 2665.
18 W. C. Swope and H. C. Andersen, *Phys. Rev. B*, 1990, **41**, 7042.
19 G. M. Torrie and J. P. Valleau, *Chem. Phys. Lett.*, 1974, **28**, 578.
20 P. J. Steinhardt, D. R. Nelson and M. Ronchetti, *Phys. Rev. B*, 1983, **28**, 784.
21 P. R. ten Wolde, M. J. Ruiz-Montero and D. Frenkel, *Phys. Rev. Lett.*, 1995, **75**, 2714.
22 P. R. ten Wolde, M. J. Ruiz-Montero and D. Frenkel, *J. Chem. Phys.*, 1996, **104**, 9932.
23 S. Pronk and D. Frenkel, *J. Chem. Phys.*, 1999, **110**, 4589.
24 D. Wright, R. Caldwell, C. Moxeley and M. S. E1-Shall, *J. Chem. Phys.*, 1993, **98**, 3356.
25 D. Wright and M. S. El-Shall, *J. Chem. Phys.*, 1993, **98**, 3369.
26 F. F. Abraham, *Science*, 1970, **168**, 833.
27 V. Talanquer and D. W. Oxtoby, *J. Chem. Phys.*, 1993, **99**, 4670.
28 P. R. ten Wolde, D. W. Oxtoby and D. Frenkel, *Phys. Rev. Lett.*, 1998, **81**, 3695.
29 P. R. ten Wolde and D. Frenkel, *J. Chem. Phys.*, 1998, **109**, 9901.
30 I. Kusaka, Z.-G. Wang and J. H. Seinfeld, *J. Chem. Phys.*, 1998, **108**, 3446.
31 A. McPherson, *Preparation and Analysis of Protein Crystals*, Krieger Publishing, Malaba, 1982.
32 S. D. Durbin and G. Feher, *Annu. Rev. Phys. Chem.*, 1996, **47**, 171.
33 F. Rosenberger, *J. Cryst. Growth*, 1996, **166**, 40.
34 A. George and W. W. Wilson, *Acta Crystallogr., Sect. D*, 1994, **50**, 361.
35 T. L. Hill, *An Introduction to Statistical Thermodynamics*, Dover, New York, 1986.
36 E. G. Richards, *An Introduction to Physical Properties of Large Molecules in Solution*, Cambridge University Press, Cambridge, 1980.
37 D. Rosenbaum, P. C. Zamora and C. F. Zukoski, *Phys. Rev. Lett.*, 1996, **76**, 150.
38 D. Rosenbaum and C. F. Zukoski, *J. Cryst. Growth*, 1996, **169**, 752.
39 M. H. J. Hagen and D. Frenkel, *J. Chem. Phys.*, 1994, **101**, 4093.
40 A. P. Gast, W. B. Russell and C. K. Hall, *J. Colloid Interface Sci.*, 1983, **96**, 251.
41 A. P. Gast, W. B. Russell and C. K. Hall, *J. Colloid Interface Sci.*, 1986, **109**, 161.
42 H. N. W. Lekkerkerker, W. C. K. Poon, P. N. Pusey, A. Stroobants and P. B. Warren, *Europhys. Lett.*, 1992, **20**, 559.
43 S. M. Ilett, A. Orrock, W. C. K. Poon and P. N. Pusey, *Phys. Rev. E*, 1995, **51**, 1344.
44 W. C. K. Poon, A. D. Pirie and P. N. Pusey, *Faraday Discuss.*, 1995, **101**, 65.
45 W. C. K. Poon, *Phys. Rev. E*, 1997, **55**, 3762.
46 C. R. Berland, G. M. Thurston, M. Kondo, M. L. Broide, J. Pande, O. O. Ogun and G. B. Benedek, *Proc. Natl. Acad. Sci. USA*, 1992, **89**, 1214.
47 N. Asherie, A. Lomakin and G. B. Benedek, *Phys. Rev. Lett.*, 1996, **77**, 4832.
48 M. L. Broide, T. M. Tominc and M. D. Saxowsky, *Phys. Rev. E*, 1996, **53**, 6325.
49 M. Muschol and F. Rosenberger, *J. Chem. Phys.*, 1997, **107**, 1953.
50 A. Kose and S. Hachisu, *J. Colloid Interface Sci.*, 1976, **55**, 487.
51 C. Smits, J. S. van Duijneveldt, J. K. G. Dhont, H. N. W. Lekkerkerker and W. J. Briels, *Phase Transitions*, 1990, **21**, 157.
52 P. R. ten Wolde and D. Frenkel, *Science*, 1997, **277**, 1975.

Paper 8/09346F